Hydrol. Earth Syst. Sci. Discuss., 5, 3213–3245, 2008
www.hydrol-earth-syst-sci-discuss.net/5/3213/2008/

Hydrology and Earth System Sciences Discussions

Papers published in *Hydrology and Earth System Sciences Discussions* are under open-access review for the journal *Hydrology and Earth System Sciences*

Calibration and sequential updating of a coupled hydrologic-hydraulic model using remote sensing-derived water stages

M. Montanari[1], R. Hostache[1], P. Matgen[1], G. Schumann[2], L. Pfister[1], and L. Hoffmann[1]

[1]Centre de Recherche Public – Gabriel Lippmann, 4422, Belvaux, Grand Duchy of Luxembourg
[2]School of Geographical Sciences, University of Bristol, BS81SS, UK

Received: 24 September 2008 – Accepted: 25 September 2008
– Published: 19 November 2008

Correspondence to: M. Montanari (montanar@lippmann.lu)

Published by Copernicus Publications on behalf of the European Geosciences Union.

Abstract

Two of the most relevant components of any flood forecasting system, namely the rainfall-runoff and flood inundation models, increasingly benefit from the availability of spatially distributed Earth Observation data. With the advent of microwave remote sensing instruments and their all weather capabilities, new opportunities have emerged over the past decade for improved hydrologic and hydraulic model calibration and validation. However, the usefulness of remote sensing observations in coupled hydrologic and hydraulic models still requires further investigations. Radar remote sensing observations are readily available to provide information on flood extent. Moreover, the fusion of radar imagery and high precision digital elevation models allows estimating distributed water levels. With a view to further explore the potential offered by SAR images, this paper investigates the usefulness of remote sensing-derived water stages in a modelling sequence where the outputs of hydrologic models (rainfall-runoff models) serve as boundary condition of flood inundation models. The methodology consists in coupling a simplistic 3-parameter conceptual rainfall-runoff model with a 1-D flood inundation model. Remote sensing observations of flooded areas help to identify and subsequently correct apparent volume errors in the modelling chain. The updating of the soil moisture module of the hydrological model is based on the comparison of water levels computed by the coupled hydrologic-hydraulic model with those estimated using remotely sensed flood flood extent. The potential of the proposed methodology is illustrated with data collected during a storm event of the Alzette River (Grand-Duchy of Luxembourg). The study contributes to assessing the value of remote sensing data for evaluating the saturation status of a river basin.

1 Introduction

Over the last decade, many studies demonstrated that spatial information on the distributed physiogeographical characteristics and hydrological responses of river basins can be gained from remote sensing observations. Taking into account satellite data in flood forecasting systems has the potential of significantly improving model performances. Indeed, the list of Earth Observation-derived products that are potentially useful in watershed modelling is long, including, most notably, precipitation fields, land use maps, digital elevation models, maps of snow cover, soil moisture, flood extent, vegetation cover and evapotranspiration. The requirements with respect to imaging frequency, spatial resolutions and accuracy strongly depend on the hydrological variables to be monitored and the basin characteristics to be mapped. Whereas some basin characteristics such as land use and topography can be retrieved from a limited amount of images, the time variation of soil moisture, flood extent and snow cover implicates that the corresponding data need to be provided at a daily or at least weekly basis in order to be routinely used in forecasting systems.

Recent studies on integrating remote sensing observations of floods with hydrodynamic models investigated the potential for calibrating friction parameters in flood models (e.g. Aronica et al., 2002; Mason et al., 2003; Werner et al., 2005). In the same general context, Schumann et al. (2007a) demonstrated the potential of Earth Observation data to understand and improve model structures by comparing remote sensing-derived water stages along a river reach with simulated water surface lines. Here we want to introduce a new approach in the framework of "predictions in ungauged basins (PUB)", initiative of the IAHS (International Association of Hydrological Sciences), which consists in using remote sensing observations of floods to update the soil moisture module of the rainfall-runoff component in a flood forecasting system. Andreadis et al. (2007) and Pappenberger et al. (2006) showed that the uncertainties associated with boundary conditions have a significant impact on inundation prediction accuracy. Moreover, they showed that remote sensing-derived water stages were useful to correct inflow data, thereby improving the skill of the hydrodynamic models. The dominant practice in hydrodynamic modelling consists in using recorded hydrographs as boundary conditions. In this case the uncertainty of the boundary condition depends on the accuracy of the stage-discharge relationship. In ungauged catchments, the associated uncertainty is increased significantly because hydrologic models need to estimate streamflow at the upstream boundary. In order to be able to simulate hydrographs accurately, these models need to predict the partitioning of precipitation into infiltration and stormflow adequately. This distribution largely depends on antecedent moisture conditions. Pfister et al. (2003) showed in a case study in a humid temperate region that stormflow coefficients may vary significantly depending on antecedent moisture conditions. These considerations have motivated many studies focusing on the remote sensing of soil moisture as the key environmental variable to be monitored in order to assess the saturation status of a river basin during storm events. As a result of all these efforts, there is nowadays a large variety of methods available to assess basin saturation via remote sensing of soil moisture. However, remote sensing observations of soil moisture are themselves subject to considerable uncertainties and thus one may question the usefulness of microwave remote sensing of soil moisture for hydrological modelling.

There is no doubt that in the active microwave domain, Synthetic Aperture Radar (SAR) shows a high sensitivity toward water content in the first few centimeters of the soil. There are numerous studies that demonstrate this relationship (e.g. Quesney et al., 2000; Le Hégarat-Mascle et al., 2002; Zribi et al., 2005). In any discussion, it is however essential to distinguish between remote sensing for small-scale soil moisture of bare soils with known characteristics and surface soil moisture monitoring over larger areas. SAR backscattering is highly dependent on topography, soil texture, surface roughness vegetation cover and soil moisture, meaning that soil moisture inversion is extremely difficult. Even in an ideal scenario where the effects due to topography, roughness and vegetation cover can be estimated, SAR generally fails to provide soil moisture variations at the small-scale (e.g. Wagner and Pathe, 2004; Walker et al., 2004). Only the averaging of the SAR signal over large areas seems to give acceptable estimates of the soil mean response. If the soil moisture response to the SAR backscatter can be separated from the vegetation contribution and assuming that soil roughness does not need to be taken into account at larger scales, one may obtain robust estimations of watershed averaged soil moisture indices (Le Hégarat-Mascle et al., 2002). But even with such a scenario, remote sensing can only be used to retrieve soil moisture in the first few centimeters of soil, whereas runoff generation is more strongly controlled by deeper layers. Despite the aforementioned limitations, some studies (Pauwels et al., 2001; François et al., 2003; Matgen et al., 2006) indicate that the integration of remote sensing observations of average basin soil humidity under certain conditions allows increasing the performance of rainfall-runoff models.

This paper considers an alternative approach to the existing studies mentioned above. Given the current limitations of microwave sensors to map soil moisture, remote sensing of floods may be regarded as an inviting alternative to assess basin saturation implicitly. As microwaves are reflected away from the sensor by smooth open water bodies, flood area detection via microwave remote sensing is rather straightforward (Smith, 1997). River stage can be estimated at the land-water interface using remote sensing derived flood boundaries in combination with topographic maps (e.g. Oberstadler et al., 1997; Schumann et al., 2007b; Hostache et al., 2007) even though associated uncertainties can be high (Schumann et al., 2008). The appraisal of surface water storage within a given river reach can be done via the subtraction of the floodplain topography from the water surface. It can be argued that the surface water volume represents the aggregate response of a river basin to a storm event. Our assumption is that time series of remote sensing images of floods allow monitoring surface water volumes and, as a matter of fact, help to estimate effective rainfall during storm events (i.e. the part of total rainfall that is routed as stormflow towards the outlet). Knowing the total rainfall amount in the contributing area, it appears sensible to use these data sets for monitoring the time variation of runoff coefficients. Our hypothesis will be tested by means of a case study that focuses on an application to the Alzette River in Luxembourg. We use this test site to establish the proof-of-concept of a routine remote sensing-based flood monitoring service as a means to monitor the saturation status of the river basin.

2 General approach

The methodology presented in this study aims at integrating remote sensing-derived information in a coupled hydrologic-hydraulic (H-H) model in order to improve model results by identifying and correcting the bias that may result from errors in the simulated inflow. The modelling sequence is performed by coupling a simplistic rainfall-runoff model and a 1-D flood propagation model so that the output of the former serves as input to the latter.

The analysis is carried out using two possible calibration approaches whereby the value of remote sensing data of floods in an aggregated modelling system will be assessed. Initially, an "all-at-once" calibration scheme is conducted. It consists in estimating both the hydrologic and the hydraulic model parameters in one go using SAR-derived water stages. Afterwards, a sequential model-updating scheme is performed in order to investigate the usefulness of remote sensing data for monitoring the saturation status of the river basin. This second approach first divides the parameters of the coupled H-H model into constants (i.e. parameters representing basin and river characteristics that can be transferred from one event to another) and time-varying (i.e. parameters whose values are event dependent). It is worth noting that the only time-varying parameter in this study is the stormflow coefficient, which implicitly represents the moisture status of the drainage area since the basin's antecedent moisture condition influences the partitioning of the total rainfall into infiltration and runoff. Then, model parameters are calibrated with field data collected during a well-documented flood event (reference event A) and the constants are transferred to another flood event (reference event B). Finally, the time-varying parameter, namely the stormflow coefficient, the value of which is expected to change from the event A to any other event, is re-calibrated for the event B using the SAR-derived water stages.

For both approaches, the calibration procedure is based on a random generation of parameter sets from within specified ranges using the Monte Carlo method. Simulations of the coupled H-H model are performed with each set of parameters. Then, outputs provided by each simulation are compared to recorded observations. Using this kind of calibration process, it is possible to represent performances or errors of the model versus parameter values.

In order to establish the value of remote sensing derived flood information for model calibration and updating, the outlined general approach will be applied on a case study in Luxembourg.

3 Study area and available data

The area of interest is located in the Grand Duchy of Luxembourg and includes the upstream part of the Alzette River basin expanding from the head of the river, 4 km south of the French-Luxembourg border, to Mersch. Since this study deals with a loose H-H model sequence, two different sub-study areas have been defined (Fig. 1): the drainage area to the stream gauge located in Pfaffenthal (Luxembourg City) and the river reach between Pfaffenthal and Mersch, respectively. The first covers a area of 356 km^2 and consists of about 50% of marls, whereas the remaining 50% is divided into loam and limestone in the upstream part of the basin and sandstone in the downstream part, close to Luxembourg City. The overall land use is 50% agricultural area, 22% urban area, 28% forest and semi-natural areas. A gauging station, operated since 1996, is located near the village of Livange, which provides cumulated precipitation amounts every 15 min. The second study area is the 19 km reach of the Alzette River between the gauging stations at Pfaffenthal and Mersch. Here, the river meanders in a relatively large and flat plain characterized by an average width of 300 m and a mean slope of 0.08%. The average channel depth is 4 m.

In this study the well-documented flood events that occurred in January 2003 and January 2007 have been investigated: the former, which is the focus of this study, is a medium sized flood event with an estimated return period of 5 years and a peak discharge of 0.78 mm/h; the latter is a rather small (estimated return period of 3.8 years) flood event characterized by a peak discharge recorded in Pfaffenthal of 0.59 mm/h.

The hydrometric data were recorded at a 15-minutes time-step at six stream gauges located in the villages of Pfaffenthal (upstream), Walferdange, Steinsel, Hunsdorf and Lintgen, but the stage hydrographs at Lintgen and Hunsdorf are only available for low water depths because of a temporary malfunctioning of the measurement system during high flows. Moreover, the maximum water level during the flood event has been measured using a theodolite (altimetric accuracy around ±2 cm) at 7 points distributed across the floodplain. The altimetric data available are a LiDAR DEM with a 2 m spatial resolution and a ±15 cm mean altimetric uncertainty, for the floodplain terrain elevations, and 200 bathymetric cross sections with a "theoretical" (some errors of more than 30 cm have been found during ground control survey) centimetric altimetric uncertainty, for the river channel elevations.

Two SAR images, acquired at two distinct stages of the 2003 flood event (Fig. 2 shows the flooded area covered by both images), have been used in this study. One has been acquired by the ERS-2 satellite during the rising limb of the flood wave. The second image was acquired by the ENVISAT satellite just after the beginning of the recession limb of the flood wave. The characteristics of these two images are summarized in Table 1.

4 Methodology

4.1 Coupled H-H model set-up

As mentioned above, the modelling sequence consists of the loose coupling of a lumped conceptual event-based rainfall-runoff (R-R) model and a 1-D hydrodynamic model. The former represents the rainfall-runoff transformation occurring in the drainage area of the Alzette River up to Pfaffenthal and uses the rainfall recorded at the rain gauge located in Livange as input data. The latter simulates the propagation of the flood wave across the river channel and floodplain between the gauging stations in Pfaffenthal and Mersch. The link between the two models in the sequence is the flood discharge hydrograph computed by the R-R model since this is integrated with the hydraulic model as upstream boundary condition.

4.1.1 Hydrologic component of the modelling sequence

A Nash cascade (Nash, 1960), based on an instantaneous unit hydrograph (IUH) model, is used to simulate the discharge of storm run-off. The equation of the IUH (pulse response function) is given as follows:

$$u(t) = \frac{1}{K\Gamma(n)} \left(\frac{t}{K}\right)^{n-1} e^{-\frac{t}{K}} \tag{1}$$

In Eq. (1), t stands for time, n is the number of reservoirs in the Nash cascade, K the storage constant and Γ the Gamma distribution function depending on K and n. By differentiating Eq. (1) with respect to t and equating to zero to consider the peak discharge, t_p (recession time scale) becomes a model parameter and the expression of K is obtained as follows:

$$K = \frac{t_p}{n-1} \tag{2}$$

As a matter of fact, the Nash cascade is described by two parameters n and t_p. Furthermore, since one of the hydrologic inputs is represented by the effective rainfall, a third parameter needs to be taken into account: the stormflow coefficient, c, defined as the ratio between stormflow and rainfall volumes. The stormflow coefficient represents an event-dependent parameter and its variability from one event to another is very difficult to assess, particularly in ungauged catchments. In humid temperate hydrological regimes of north western Europe, the dominant runoff-generating process is saturation overland flow and is the result of near-surface saturation conditions. The rainfall-infiltration-runoff partitioning, represented in the simplistic 3-parameter model by the value of c, obviously largely depends on the antecedent moisture conditions. Pfister et al. (2003) found a linear relationship between basin water balance and runoff coefficients for the same catchment supporting that the ratio between stormflow and rainfall reflects the actual degree of saturation of the basin and it is not significantly influenced by the total amount of rainfall (Pfister et al., 2002).

The Nash cascade model allows computing flood discharge hydrographs using as inputs hourly effective rainfall, assumed to be uniformly distributed in space over a defined period of time, and as hydro-morphological characteristics the basin surface and the base flow. As the total volume of rainfall gives the discharge of storm run-off, the base flow is added to generate the flood hydrograph that takes into account both the storm event and the discharge at the time t_0 when rainfall starts. In this study the base flow is supposed to be constant during the flood event.

4.1.2 Hydraulic component of the modelling sequence

Since in the area between Pfaffenthal and Mersch the flow direction is mainly parallel to the channel, the 2-D flow field that is typically related to riverbank overtopping can be accurately approximated by a 1-D representation (i.e. velocity components in directions other than the main flow directionare not accounted for). Therefore the widely used Hydrologic Engineering Center River Analysis System – HEC-RAS – was set-up for river flow computation. The HEC-RAS model (HEC-RAS 4.0, 2008), developed by the Hydrologic Engineering Center belonging to the US Army Corps of Engineers, allows 1-D steady and unsteady flow calculations. The unsteady flow equation solver, UNET (Barkau, 1992), simulates 1-D unsteady flow through a full network of open channels. Setting up HEC-RAS requires a three-dimensional (3-D) geometry of the floodplain and channel, initial as well as boundary conditions, and hydraulic parameters (e.g. friction coefficients). In the studied river reach the channel and floodplain topography are represented by 172 3-D cross sections, placed perpendicularly to the flow direction, derived from the LiDAR DEM and the bathymetric data. The boundary conditions of the model are as follows:

– upstream: the flow hydrograph at the hydrometric station in Pfaffenthal (R-R model output);

– downstream: the normal depth.

Furthermore, two tributaries – the Eisch and Mamer rivers – have their confluences with the Alzette River between two model cross sections, upstream of the town of Mersch. Nevertheless, since their contribution is not relevant for the flood extent information within the study area, the downstream boundary of the hydraulic model is defined upstream of the confluences, in order to simplify the analysis and restrain the number of inflows.

The initial condition is calculated by the model as a steady flow simulation using the discharge at Pfaffenthal gauging station (upstream boundary) at t_0.

As mentioned above, the implementation of a hydraulic model also requires the specification of roughness parameters: two Manning friction coefficients, one for the river channel, n_c, and one for the floodplain, n_{flp}, are considered. A single channel Manning coefficient is attributed to the entire reach in the model, as the channel aspect appeared homogeneous along the study area during field observations. Moreover, for the Alzette reach, Schumann et al. (2007a) demonstrate that a high number of acceptable flood simulations can be obtained at the reach-scale without spatially distributing channel roughness.

4.2 Water level estimation from remote sensing observation

The water level estimation methodology is described in details in (Hostache et al., 2007, 2008). It is composed of two main steps: i) SAR image processing in order to extract the flood extent limits that are relevant for water level estimation, ii) estimation of water levels by merging the relevant limits and a high resolution high accuracy Digital Elevation Model (DEM) under hydraulic coherence constrains. In the first step of this method, the flood extent is derived from the SAR image using radiometric thresholding. It is worth noting that this SAR image derived flood extent may be prone to local misclassifications that are mainly due to emerging objects that may mask water. As a matter of fact, some flood extent limits may be erroneous. Since the water levels are estimated by merging the flood extent limits and the DEM, these erroneous limits, when taken into account, induce errors on the resulting water level estimates. As a consequence, it has been chosen to remove from the flood extent limits those parts that are located in the vicinity of trees or buildings (mapped using aerial photographs and land use maps). The remaining limits, called "relevant" limits hereafter, shaped as small patches spatially distributed across the floodplain, will be used for water level estimation.

In the second step the "relevant" limits are merged with the underlying DEM in order to extract, for each pixel of these limits, the terrain elevation. It is worth noting that the DEM altimetric uncertainty and the flood extent limits spatial uncertainty are taken into account during this merging. Next, by affecting the relevant limit pixels with cross sections of the hydraulic model geometry using a snapping distance equal to the mean cross section spacing, it is possible to estimate, for some model cross sections, water levels as intervals $IWL_i^{\mathrm{sat}} = \left[WL_{\mathrm{min},i}^{\mathrm{sat}}; WL_{\mathrm{max},i}^{\mathrm{sat}}\right]$ (since numerous pixels of the relevant limits and thus numerous terrain elevation values are affected to a cross section). These intervals constitute primary water level estimates. Furthermore, it has been shown (Hostache et al., 2008) that these water level estimates have to be hydraulically constrained for more efficiency in the framework of hydraulic model calibration. Previously introduced by Raclot (2003), the hydraulic coherence constraints impose a decrease of the water level from upstream to downstream, when the flow velocity is rather low (which is true for the Alzette river). Applied to the intervals of water level estimation, these constraints force a decrease upon the maxima ($WL_{\mathrm{max},i}^{\mathrm{sat}}$) from upstream to downstream and an increase upon the minima ($WL_{\mathrm{min},i}^{\mathrm{sat}}$) from downstream to upstream. This provides constrained water level estimates $IWL_i^{\mathrm{sat}} = \left[WL_{\mathrm{min},i}^{\mathrm{sat}}; WL_{\mathrm{max},i}^{\mathrm{sat}}\right]$, called SAR derived water levels hereafter, that will be integrated with the calibration process.

4.3 The value of SAR-derived water stages within an "all-at-once" calibration scheme

As a first approach, the calibration of the modelling sequence is performed using a Monte Carlo approach: each randomly generated parameter set contains three hydrologic (c, t_p, n) and two hydraulic parameters (n_c, n_{flp}) and allows running a simulation. It is worth mentioning that all parameters except one are closely related to basin characteristics and can be considered constants. The stormflow coefficient, however, is an event-dependent parameter, although Pfister et al. (2002) found that, for the same catchment, this value remains rather constant during winter and summer months and abruptly switches values in spring and autumn.

The final output of the H-H model, i.e. the simulated water levels, is compared to water levels estimated by the SAR flood images. Each simulation is stopped at time step t_{sat} of the satellite overpass and simulated water levels are considered as matching the observations if they fall inside the interval of SAR water levels ($WL^{sat}_{min,i}<WL^{sim}_{i,t_{sat}}<WL^{sat}_{max,i}$). It is worth noting here that, for the sake of simplification, all model runs inside the intervals are given a score of 1.

For each set of parameters the following performance criterion has been defined:

$$P_{sat}=\sum_{i=1}^{N}\left(\frac{\Delta WL_i}{N}\right) \text{ where } \Delta WL_i=\begin{Bmatrix} 1 \text{ if } WL^{sim}_{i,t_{sat}} \in IWL^{sat}_i \\ 0 \text{ if } WL^{sim}_{i,t_{sat}} \notin IWL^{sat}_i \end{Bmatrix} \tag{3}$$

In (3), $WL^{sim}_{i,t_{sat}}$ is the simulated water level at the satellite overpass, IWL^{sat}_i=[$WL^{sat}_{min,i}$; $WL^{sat}_{max,i}$] is the interval of the remote sensing derived water level on the model cross section i, and N is the number of model cross sections where a SAR water level is available. This performance criterion provides, for each model run (i.e. for each set of parameters), the number of cross sections (expressed as a fraction of the total), at which the simulated water level matches the observations.

4.4 The value of SAR-derived water stages within a sequential updating scheme

For the second calibration approach, variable parameters are separated from those that are assumed not to vary from one flood event to another. As a matter of fact, the parameters that are related to constant basin characteristics are calibrated using field observations of a first flood event, then transferred to another event for which SAR water stages are available.

As mentioned earlier, c is the only variable parameter within the hydrologic model since it depends on the soil moisture conditions that control rainfall-infiltration-runoff partitioning, whereas n and t_p are related to the physiogeographical characteristics of the basin.

With respect to the hydrodynamic parameters, it is sensible to assume that, from a certain water stage onward, channel roughness does not vary in time, unless significant changes occur inside the river bed.

4.4.1 Calibration of model parameters using field observations

Since the presented H-H model is based on a loose coupling, it is sensible to use a first flood event to calibrate the hydrologic and the hydraulic model components independently.

The widely used Nash criterion (Nash and Sutcliffe, 1970) is applied to assess the performance of the hydrologic model. The flow hydrograph simulated by the Nash cascade at the outlet of the study drainage area is compared to the flow hydrograph observed in Pfaffenthal (with this definition the authors refer to the flow hydrograph calculated using the observed stage hydrograph and the rating curve).

$$\text{Nash} = 1 - \frac{\sum_{t=t_0}^{t_{\text{end}}} \left(Q_{\text{sim}}(t) - Q_{\text{obs}}(t)\right)^2}{\sum_{t=t_0}^{t_{\text{end}}} \left(Q_{\text{sim}}(t) - \overline{Q_{\text{obs}}}\right)^2} \quad (4)$$

In Eq. (3) $Q_{\text{obs}}(t)$ and $Q_{\text{sim}}(t)$ are the observed and simulated discharge at time t, respectively. t_o and t_{end} are the starting and ending simulation time; $\overline{Q_{\text{obs}}}$ is the observed mean discharge between t_o and t_{end}. The Nash criterion represents the percentage of the observed discharge variance explained by the model.

In order to calibrate the hydraulic model, the observed flow hydrograph is used as the upstream boundary condition. The objective function for the hydraulic model is the root mean squared error (RMSE) between the simulated and observed water stages at six hydrometric stations along the river reach.

$$\text{RMSE}_{\text{global}} = \sqrt{\sum_{i=0}^{N\_hs} \frac{\left(\sum_{t=t_0}^{t_{\text{end}}} (H_{\text{sim}}(t) - H_{\text{obs}}(t))^2\right)(i)}{N(i)}} \tag{5}$$

In Eq. (4) $H_{\text{obs}}(t)$ and $H_{\text{sim}}(t)$ are the observed and simulated water levels at time t, respectively. t_o and t_{end} are the starting and ending simulation time, $N(i)$ is the number of measures of water level recorded at the hydrometric station i. The RMSE is equal to 0 if the observed and simulated hydrographs fit perfectly and the more divergent these hydrographs, the higher the RMSE.

4.4.2 Re-calibration of the stormflow coefficient using SAR images

The next step of the methodology aims at assessing the saturation status of the river basin in order to reduce the volume errors in the simulated inflow, namely the flow hydrograph in Pfaffenthal, using the remote sensing-derived water levels. To achieve this goal the modelling sequence is set-up using the values of the hydrologic parameters n and t_p and the Manning coefficients found for the event used in Sect. 4.4.1 and the stormflow coefficient is re-calibrated for another event using remote sensing observations.

The evaluation procedure is the same as the one described in the Sect. 4.3 and the performance P_{sat} (see Eq. 3) represents, for each value of c, the number of cross sections (expressed as a fraction of the total), at which the simulated water level matches the observations.

Additionally, stormflow coefficients giving water levels within the uncertainty interval of SAR-derived water stages (IWL_i^{sat}) are plotted for each cross section over the entire reach. This "local" evaluation gives an appreciation of the variability of likely c values depending on which cross section is considered and represents a helpful tool to better understand the results obtained with the previous "global" evaluation.

5 Results and discussion

5.1 Water level estimation from remote sensing observation

The water level estimation method presented in part 4.2 has been applied to the ERS and the ENVISAT images using the LiDAR DEM as source of terrain elevation data. To characterize the uncertainty of the resulting water levels, the half mean range $\frac{\text{mean}(WL_{max}-WL_{min})}{2}$ of the intervals of water level has been calculated. This "mean uncertainty" is equal to ±43 cm for the ERS image and ±54 cm for the ENVISAT image. Furthermore, since the ENVISAT image has been acquired close to peak discharge, the ENVISAT-derived water levels have been compared to seven ground measured high water marks (see Sect. 2). This comparison shows the reliability of the water level estimation method since all these high water marks are included inside the intervals of SAR-derived water levels. This result validates the hypothesis of the method stating that the real water level is included inside SAR-derived water levels.

5.2 The "all-at-once" calibration scheme

The aim of the first calibration approach was to verify the capability of remote sensing-derived water levels to allow the calibration of the coupled H-H model for the January

2003 event in one go.

To set up the hydrologic model, hourly rainfall data observed in Livange between the 1st and 7th of January 2003 were used. The surface area of the basin (356 km^2) and the base flow measured in Pfaffenthal at the beginning of the storm event (0.11 mm/h) also served as input to the hydrologic model.

The hydrodynamic model was set up as proposed in Sect. 4 with the upstream boundary condition being output by the hydrologic model and the downstream boundary condition being the normal depth.

For the calibration procedure, 3000 sets of parameters were randomly generated within the following intervals of physically plausible values:

- for the stormflow coefficient: $c \in [0.1; 0.9]$;
- for the number of reservoirs: $n \in [1.1; 5]$;
- for the recession time scale: $t_p \in [1; 30]$;
- for the channel Manning coefficient: $n_c \in [0.01; 0.1]$;
- for the floodplain Manning coefficient: $n_{\mathrm{flp}} \in [0.01; 0.2]$.

For each generated set of parameters, one run of the modelling chain was performed for the period between the 1st and 7th of January 2003.

The calibration was performed using both the ENVISAT and the ERS-2 images. In both cases, the comparison between simulated and remote sensing-derived water levels did not provide satisfactory results since none of the parameters became identifiable. According to the equifinality concept (Beven, 2006), this means that due to correlated model parameters, numerous parameter sets give similar performances with respect to the reference data at hand. This phenomenon is due to the fact that a decrease of c leads to a decrease of the discharge but at the same time an increase of the roughness value leads to an increases of the water level. This result highlights the necessity to reduce the number of parameters to be calibrated. Two snap shots of flood extent derived from satellite imagery do not contain enough information to unambiguously calibrate a multitude of model parameters. This result is well in line with previous studies on the same river reach demonstrating the equifinality phenomenon in hydrodynamic model calibration with remote sensing-derived flood information (e.g. Hostache et al., 2007). To circumvent this problem the number of flood images needs to be increased and complementary data sets need to be considered for model calibration.

5.3 The sequential updating scheme

The second approach focuses on estimating the saturation status of the river basin by distinguishing between event-dependent and constant parameters. As a matter of fact the values of n and t_p calibrated using the 2007 event can be transferred to the 2003 test event, as well as the calibrated values of the roughness, whereas the parameter c needs to be re-calibrated, as it is event-specific and expresses indirectly the soil moisture conditions during the 2007 flood event. To validate the hypothesis of n and t_p being invariant in time, a test has been done with the rainfall-runoff data recorded during five additional events. The Nash cascade algorithm was run for each test event using the same n and t_p found for 2007 and varying only c in order to optimize the model results. The analysis of the performances obtained comparing the observed and the simulated flow hydrographs (see Table 2) leads to the conclusion that it is sensible to support the transferability of n and t_p from one event to another.

The Nash cascade was set up using as input the hourly rain data observed in Livange between the 17th and the 25th of January 2007 and a base flow in Pfaffenthal of 0.06 mm/h. Then, 10 000 sets of hydrologic parameters were randomly generated within the same intervals as those used for the all-at-once scheme and for each set, one run of the hydrologic model was performed. Then, for each run, the computed flow hydrograph is compared with the one observed in Pfaffenthal using the Nash coefficient as a measure of model performance. The parameter set giving the best fit (Fig. 3) with a Nash efficiency of 0.95 provides c=0.73, n=1.71 and t_p=12.11 h.

The hydraulic model was set up using the 2007 flood event data. For the calibration, 1000 parameter sets were randomly generated within the friction intervals defined in Sect. 5.2. Next, for each generated set of parameters, one hydraulic model run was performed for 2007 and the results were compared with field observations. For this flood event, stage hydrograph records in Pfaffenthal (upstream) Walferdange, Steinsel, Hunsdorf and Lintgen were available. As a performance criterion, a global RMSE, taking into account all five hydrometric stations, was used. The hydraulic parameters set giving the best fit at the majority of the stations (see Fig. 4) was n_c=0.047; n_{flp}=0.184. These estimates are supported by an evaluation based on an empirical approach suggested by Arcement et al. (1984) for 1-D open channel flow. The methodology is based on a step-by-step procedure, where a base value of roughness is assigned and some adjustments for various roughness factors are made in order to obtain a final value. As it is assumed that the river bed did not change significantly over the last years, it is sensible to retain the roughness values of the 2007 event for the 2003 test event.

After calibrating the coupled H-H model on the 2007 event, the parameter values obtained are transferred to the 2003 event, except for c, as it is event-specific and needs to be re-calibrated using the SAR-derived water stages:

- hydrologic parameters: n=1.71, t_p=12.11 h;
- hydraulic parameters: n_c=0.047, n_{flp}=0.184.

1000 values of c were randomly generated within the interval [0.1; 0.9] and for each value one run of the modelling sequence was performed for the January 2003 event (1–7 January).

Figure 5a and b compares water lines simulated by the model for the whole range of stormflow coefficients and the ERS-2 and ENVISAT-derived water levels. For both images, the uncertainty related to the SAR-derived water levels is of the same order of magnitude than the spread of water surface lines simulated with different values of c.

Figure 6a and b shows dotty plots of the performance P_{sat} (see Eq. 3) for the ENVISAT and ERS-2 images. In these pictures each dot corresponds to the evaluation of the model result for one value of c. The higher P_{sat}, the higher the number of cross sections providing simulated water stages matching the observations. Due to the uncertainty related to the remote sensing-derived water levels both plots are not peaky but almost flat at the top. In other words, a straightforward evaluation and identification of a "best" value of c is not really possible. However, using this "global" (reach-scale) evaluation, it is possible to significantly constrain the range of likely values of c with respect to the whole interval of physically plausible values. When comparing the water levels derived from the ENVISAT image with those simulated by the model, the values of c within the interval [0.80; 0.81] all give the best score (P_{sat}=0.84). Using the ERS-2 image, performances decrease drastically but it is still possible to identify the range of c giving the best result: [0.68; 0.86] with P_{sat}=0.58.

To validate these results the actual value of the stormflow coefficient was calculated by simply dividing the volume of runoff by the volume of rainfall, obtaining c=0.71. With respect to this value, the ENVISAT image leads to an overestimation of c, but it is worth noting that its corresponding performance (P_{sat}=0.80) is very close to the maximum. Using the ERS-2 image, the range of c giving the best performance is less constrained with respect to that obtained by ENVISAT, and the actual c value falls inside. In order to better understand the previous results, a "local" evaluation has been performed: Fig. 7a and b shows the ranges of likely c values corresponding to each cross section estimated with the ENVISAT and the ERS-2 images. The same observations can be done for both SAR images by means of a visual analysis of the results. For the majority of the cross-sections the "likely" intervals are quite wide. There is no doubt that this is due to the fact that the SAR images are affected by too much noise and consequently the uncertainty related to the water level estimation is significant. Moreover, it is clearly visible that there are some contradictions comparing results for various cross-sections: it is possible to observe that the ranges of likely values of c are totally disjoined whereas they should overlap at least in a small part in order to be coherent. This phenomenon is probably due to local errors in the model and in the data.

6 Conclusions and outlooks

This paper has presented an innovative approach to calibrate a loosely coupled hydrologic-hydraulic (H-H) model using SAR-derived water stages. Instead of using water stage data from spaceborne radar to calibrate effective roughness coefficients for the hydraulic model as has been done in previous studies, this study introduces a stepped scheme for calibration of coupled H-H models with SAR water stages whereby an aggregated variable of the basin saturation status, namely the stormflow coefficient, can be re-calibrated when referred to a different event. Results show that this approach is preferable to a more traditional "all-at-once" calibration approach given the high level of uncertainty that is associated with current satellite SAR data. Moreover, it is shown that, although a "global" evaluation does not lead to the identification of one "best" value of the stormflow coefficient, it allows to estimate a constrained range of values all giving the best performance and being reasonably close to the actual value. Furthermore, it is believed that multiple images of the same event acquired at different times help for cross-validating the results.

Although the approach proposed could be viewed as controversial with respect to existing studies that use remote sensing-derived soil moisture for hydrologic model updating because one aggregated hydrological variable has been re-calibrated with data that might not be directly comparable as such. However, these data are not totally incomparable because flood extent implicitly represents the readiness of a basin to generate runoff. As a matter of fact the saturation status of a basin controls the partitioning of rainfall into infiltration and runoff. Hence, the monitoring of surface water volumes in the river reach using SAR-derived water levels allows inferring the antecedent soil moisture conditions of the river basin. Thus, the methodology suggested might be seen as a first step toward a systematic remote sensing-based surface water monitoring system that may quasi-continuously provide valuable information for sequentially updating coupled H-H models. The authors believe that they introduced a potentially useful calibration scheme for more complex modelling sequences where highly complex parameter interaction dictates the way models need to be calibrated. More traditional calibration may fail and thus more application- and model-specific schemes are required. It is now widely recognised that (spaceborne) remote sensing offers ways to advance our understanding of natural processes and models and their evaluation. There is also little doubt that newly launched higher resolution satellites will further increase this support. However, more research is needed to better understand (i) how model parameters really interact and lead to an aggregated response (which we observe) and (ii) what information content in remotely sensed images is really needed to help achieve this.

Acknowledgements. This study was carried out in the framework of the "Hydrasens" project, funded by the National Research Fund (FNR) of the G. D. of Luxembourg and the STEREO II research program for Earth Observation of the Belgian Federal Science Policy Office (BELSPO).

References

Andreadis, K. M., Clark, E. A., Lettenmaier, D. P., and Alsdorf, D. E.: Prospects for river discharge and depth estimation through assimilation of swath-altimetry into a raster-based hydrodynamics model, Geophys. Res. Lett., 34, L10403, doi:10.1029/2007GL029721, 2007.

Arcement Jr., G. J. and Schneider, V. R.: Guide for selecting Manning's roughness coefficients for natural channels and floodplains, http://www.fhwa.dot.gov/bridge/wsp2339.pdf, 1984.

Aronica, G., Bates, P. D., and Horritt, M. S.: Assessing the uncertainty in distributed model predictions using observed binary pattern information within GLUE, Hydrol. Process., 16, 2001–2016, 2002.

Barkau, R. L.: One-dimensional unsteady flow through a full network of open channels, (Computer Program), UNET, St. Louis, MO, 1992.

Beven, K.: A manifesto for the equifinality thesis, J. Hydrol., 320, 18–36, 2006.

François, C., Quesney, A., and Ottle, C.: Sequential assimilation of ERS-1 SAR data into a coupled land surface-hydrological model using an extended kalman filter, Hydrometeorology, 4, 473–487, 2003.

HEC-RAS 4.0: http://www.hec.usace.army.mil/software/hec-ras/documents/HEC-RAS_4.0_Reference_Manual.pdf, last access: 5 May 2008.

Hostache, R., Schumann, G., Puech, C., Matgen, P., Hoffmann, L., and Pfister, L.: Water level estimation and reduction of hydraulic model calibration uncertainty using satellite SAR images of flood, BiogeoSAR, Bari, Italy, 25–28 September, 2007.
Hostache, R., Matgen, P., Schumann, G., Puech, C., Hoffmann, L., and Pfister, L.: Water level estimation and reduction of hydraulic model calibration uncertainties using satellite SAR images of floods, IEEE T. Geosci. Remote, in press, 2008.
Le Hégarat-Mascle, S., Zribi, M., Alem, F., Weisse, A., and Loumagne, C.: Soil moisture estimation from ERS/SAR data: Toward and operational methodology, IEEE T. Geosci. Remote, 40(12), 2647–2658, 2002.
Mason, D. C., Horritt, M. S., Dall'Amico, J. T., Scott, T. R., and Bates P. D.: Floodplain friction paramterization in two-dimensional river flood models using vegetation heights derived from airborne scanning laser altimetry, Hydrol. Process., 17, 1711–1732, 2003.
Matgen, P., Henry, J. B., Hoffmann, L., and Pfister, L.: Assimilation of remotely sensed soil saturation levels in conceptual rainfall-runoff models, in: Predictions in Ungauged Basins: Promises and Progress, Proceedings of symposium S7 held during the Seventh IAHS Scientific Assembly, Foz do Iguaçu, Brazil, April 2005, IAHS Publications, 303, 226–234, 2005.
Nash, J. and Sutcliffe, J.: River flow forecasting through conceptual models, 1. A discussion of principles, J. Hydrol., 10, 282–290, 1970.
Nash, J.: A unit hydrograph study with particular reference to British catchments, P. I. Civil. Eng., 17, 249–282, 1960.
Oberstadler, R., Hönsch, H., and Huth D.: Assessment of the mapping capabilities of ERS-1 SAR data for flood mapping: a case study in Germany, Hydrol. Process., 10, 1415–1425, 1997.
Pappenberger, F., Matgen, P., Beven, K., Henry J. B., Pfister, L., and de Fraipont, P.: Influence of uncertain boundary conditions and model structure on flood inundation predictions, Adv. Water Resour., 29, 1430–1449, 2006.
Pauwels, V. R. N., Hoeben, R., Verhoest, N. E. C., and De Troch, F. P.: The importance of the spatial patterns of remotely sensed soil moisture in the improvement of discharge predictions for small-scale basins through data assimilation, J. Hydrol., 251, 88–102, 2001.
Pfister, L, Drogue, G., El Idrissi, A., Humbert, J., Iffly, J. F., Matgen, P., and Hoffmann, L.: Predicting peak discharge through empirical relationships between rainfall, groundwater level and basin humidity in the Alzette River basin, Grand-Duchy of Luxembourg, Journal of Hydrology and Hydromechanics, 53(3), 210–220, 2003.

Pfister, L., Iffly, J. F., Hoffmann, L., and Humbert J.: Use of regionalized stormflow coefficients with a view to hydroclimatological hazard mapping, Hydrolog. Sci. J., 47(3), 479–491, 2002

Quesney, A., Le Hégarat-Mascle, S., Tacomnet, O., Vidal-Madjar, D., Wigneron, J. P., Loumagne, C., and Normand, M.: Estimation of watershed soil moisture index from ERS/SAR data, Remote Sens. Environ., 72, 290–303, 2000.

Raclot, D. and Puech, C.: What does AI contribute to hydrology? Aerial photos and flood levels, Appl. Artif. Intell., 17, 1, 71–86, 2003

Schumann, G., Matgen, P., Hoffmann, L., Hostache, R., Pappenberger F., and Pfister, L.: Deriving distributed roughness values from satellite radar data for flood inundation modelling, J. Hydrol., 344, 96–111, 2007a.

Schumann, G., Matgen, P., Pappenberger, F., Hostache, R., Puech, C., Hoffmann, L., and Pfister, L.: High resolution 3-D flood information from radar for effective flood hazard management, IEEE T. Geosci. Remote, 45, 1715–1725, 2007b.

Schumann, G., Matgen, P., and Pappenberger, F.: Conditioning water stages from satellite imagery on uncertain data points, IEEE Geosci. Remote S., in press, 2008.

Smith, L. C.: Satellite remote sensing of river inundation area, stage and discharge: a review, Hydrol. Process., 11, 1427–1439, 1997.

Wagner, W. and Pathe, C.: Has SAR failed in soil moisture retrieval?, in: Proceedings of the ENVISAT & ERS Symposium, Salzburg, Austria, 6–10 September, 2004.

Walker, J. P, Houser, P. R., and Willgoose, G. R.: Active microwave remote sensing for soil moisture measurement: a field evaluation using ERS-2, Hydrol. Process., 18(11), 1975–1997, 2004.

Werner, M., Blazkova, S., and Petr, J.: Spatially distributed observations in constraining inundation modeling uncertainties, Hydrol. Process., 19(16), 3081–3096, 2005.

Zribi, M., Baghdadi, N., Holah, N., and Fafin, O.: New methodology for soil surface moisture estimation and its application to ENVISAT-ASAR multi-incidence data inversion, Remote Sens. Environ., 96(3–4), 485–496, 2005.

Table 1. Characteristics of the ENVISAT and ERS-2 images.

Satellite	Band	Polarization	Pixel spacing	Georeferencing error	Acquisition date
ENVISAT	C	Vertical-Vertical (VV) Vertical-Horizontal (VH)	12.5 m	1pixel	2 January 2003 21:57
ERS-2	C	Vertical-Vertical (VV)	12.5 m	1 pixel	2 January 2003 11:00

HESSD
5, 3213–3245, 2008

HESSD

5, 3213–3245, 2008

SAR data in coupled hydrologic-hydraulic models

M. Montanari et al.

Table 2. Results of the test for the transferability of n and t_p.

Flood event	Total rainfall (mm)	Peak discharge (mm/h)	Nash coefficient
February 1997	54.48	0.592	0.949
November 1998	25.32	0.557	0.709
December 1999 (I)	65.7	0.549	0.916
December 1999 (II)	61.53	0.567	0.917
January 2001	47.85	0.685	0.903

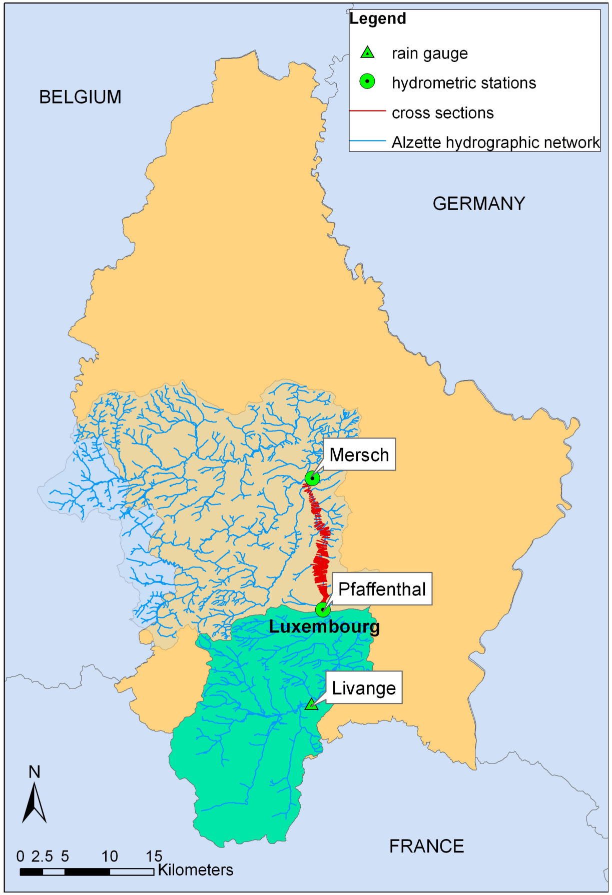

Fig. 1. The two study sites in the Alzette river basin: the drainage area to Pfaffenthal (green) and the river reach between the hydrometric stations at Pfaffenthal and Mersch whose geometry is represented by the cross sections (red lines).

HESSD

5, 3213–3245, 2008

SAR data in coupled hydrologic-hydraulic models

M. Montanari et al.

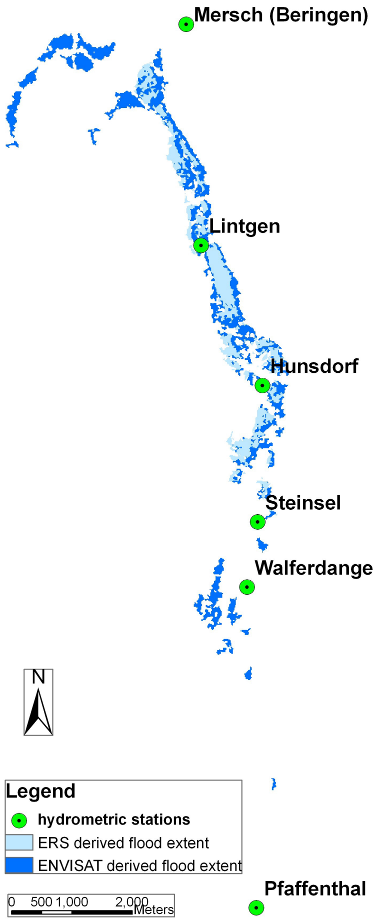

Fig. 2. Flood extents derived by the ENVISAT image (blue) and the ERS-2 image (light blue).

HESSD

5, 3213–3245, 2008

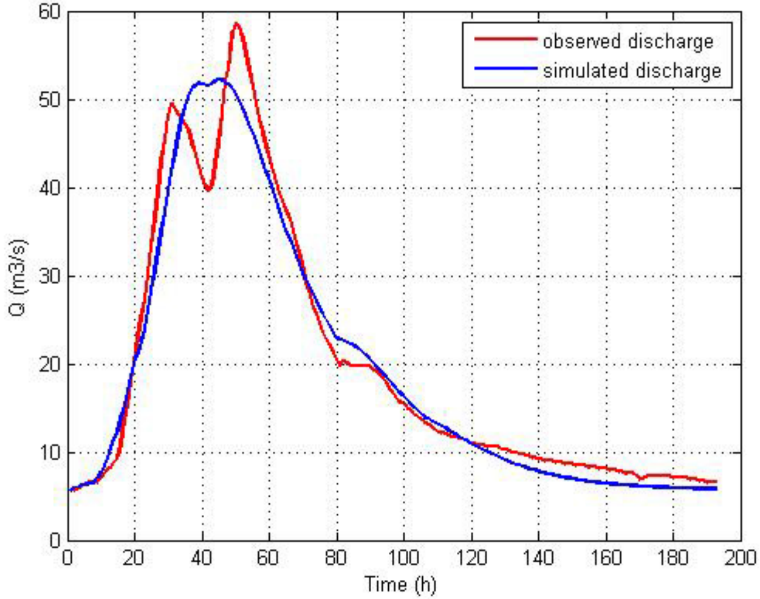

Fig. 3. Observed and simulated flow hydrograph at Pfaffenthal for the 2007 flood event.

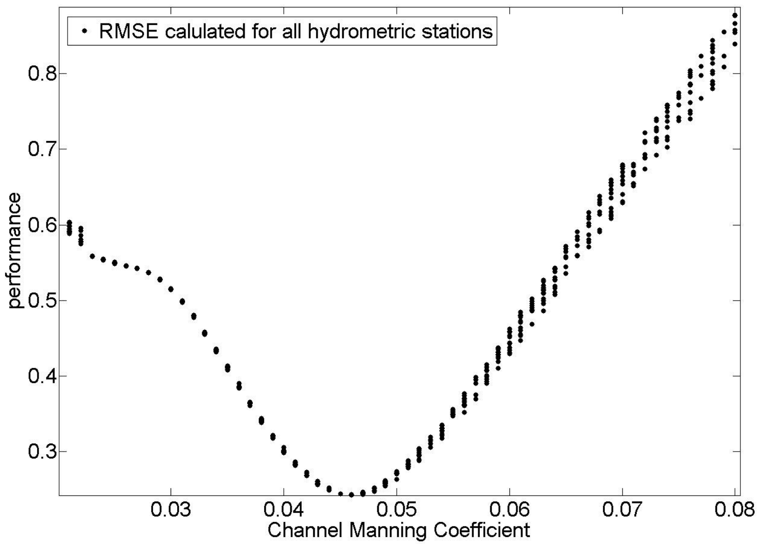

Fig. 4. Dotty plot of the model result evaluation using the RMSE calculated for all the hydrometric stations.

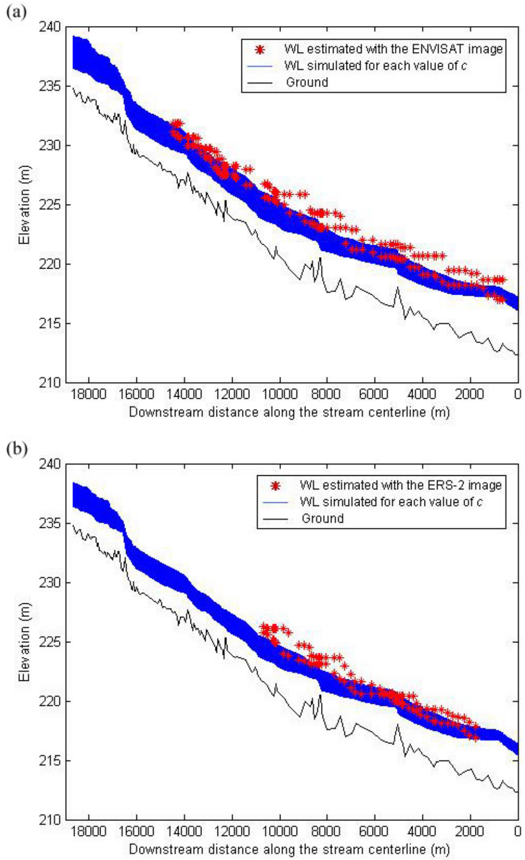

Fig. 5. Simulated water surface lines compared with the water levels estimated using the ENVISAT **(a)** and the ERS-2 **(b)** images.

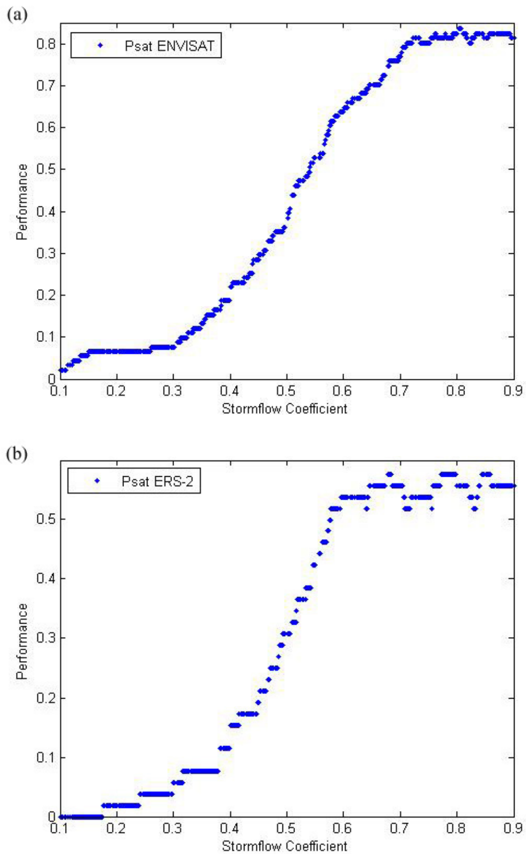

Fig. 6. Dotty plot of the "global" evaluation obtained from the ENVISAT **(a)** and the ERS-2 **(b)** image.

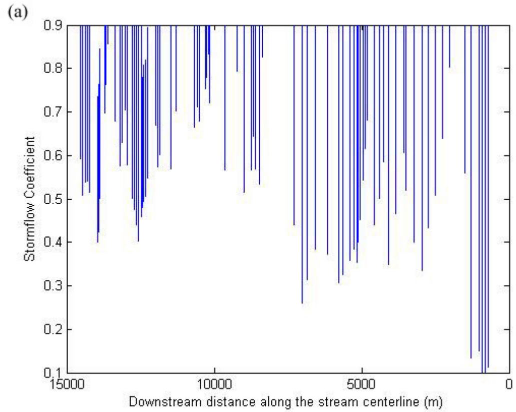

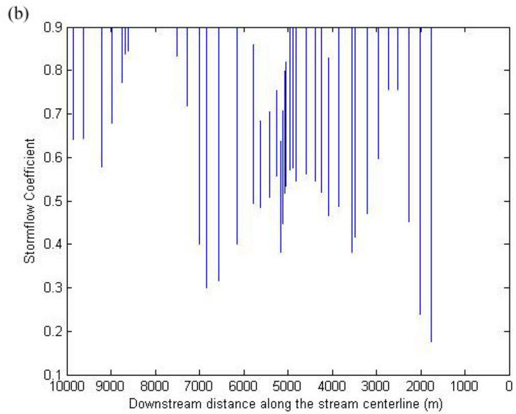

Fig. 7. "Local" evaluation using the ENVISAT **(a)** and the ERS-2 **(b)** images: blue lines represent the values of c giving simulated water levels within the uncertainty interval of SAR-derived water stages for each cross section.